Automated optical monitoring wavelength selection for thin-film filters

JANIS ZIDELUNS,[1] FABIEN LEMARCHAND,[1] DETLEF ARHILGER,[2] HARRO HAGEDORN,[2] AND JULIEN LUMEAU[1,*]

1. *Aix Marseille Univ, CNRS, Centrale Marseille, Institut Fresnel, F-13013 Marseille, France*

2. *Bühler Leybold Optics, Alzenau, Germany*

* julien.lumeau@fresnel.fr

Abstract: In this paper we study the wavelength selection process for optical monitoring of thin film filters. We first discuss the technical limitations of monitoring systems as well as the criteria defining the sensitivity of different wavelengths to thickness errors. We then present an approach that considers the best monitoring wavelength for each individual layer with a monitoring strategy selection process that can be fully automated. We finally validate experimentally the proposed approach on several optical filters of increasing complexity. Optical interference filters with close to theoretical performances are demonstrated.

Keywords: thin film optical monitoring, magnetron sputtering, optical filter

1. Introduction

Increasing stability of deposition systems has boosted the complexity of optical filter designs and hence precise control of the deposited layer thickness is required. Optical monitoring has proven to be the most reliable monitoring method at least for transparent non absorbing layers. In this paper we discuss ideas on the use of wide wavelength range for monochromatic monitoring. Our research combines and extends two already published ideas about wavelength selection process. We combine the idea of selecting wavelength by its sensitivity to thickness errors [1] with aim to automatically select monitoring wavelengths for each layer [2].

Several monitoring algorithms can be implemented in monochromatic optical monitoring systems. Turning point monitoring that relies on the detection of zero derivative is known to allow error self-compensation [3] at the monitoring wavelength. Another technique called level cut monitoring [4] relies on the detection of some predefined transmittance levels and can benefit from correction algorithms and offers a wide range of new opportunities since it becomes possible to define a larger number of possible monitoring wavelengths compared to turning point monitoring. As an example, level cut monitoring can be successfully used for dielectric quarter wave mirror deposition where turning point monitoring is usually seen as go-to method [5]. Although it has its limitations, interest in broadband optical monitoring has also increased in recent years [6, 7]. It has been reported that broadband optical monitoring can benefit from error compensation [8] but to a lesser extent than monochromatic monitoring.

To fully use benefits of error compensations or corrections, it is important to monitor all the layers on a single witness glass. However, it can be shown that in this case (direct optical monitoring), the thickness error accumulation increases with the increasing thickness and complexity of the design. In extreme situations, the observed optical signals can even become contradictory with the theory. To overcome this limitation, it is therefore of interest to perform indirect optical monitoring and use multiple witness glasses [9], changing the witness glass as soon as the error compensation is no longer valid. When performing indirect optical monitoring, layer thicknesses are controlled on several witness glasses, and therefore error compensations are possible only on individual witness level, but not for whole filter, in contrast to direct monitoring. However, the choice of changing the witness glass is generally performed empirically.

The main difficulty related to optical monitoring is that each time a new thin-film design is introduced, a new monitoring strategy must be developed. Broadband optical monitoring, whether performed as real time monitoring of thicknesses – finding the best fit for the physical thickness after each substate revolution [10] or used as a spectral measurement to determine when to stop deposition by pre-defined merit value between theory and real time spectral measurement [11] is sometimes seen as a smart solution as it does not require optical monitoring strategy; however, one drawback is related to a usually poor spectral resolution, and the increasing discrepancy between theory and measurements can make it difficult to control coatings with a high number of layers. Recent publication proposed that some sort of mix of both - monochromatic optical monitoring and broad band monitoring could provide best monitoring strategies [6].

For monochromatic monitoring, there is, as of today, no universal automatic way to determine the optimal strategy. Therefore, the choice of strategy mainly depends on the experience of the operator. One commonly used approach is to visually evaluate potential monitoring curves at different wavelengths and then use simulation software to validate strategy. Some work has already been done to help operators with automated monitoring wavelength selection [2]. When determining an optical monitoring strategy, one generally tries to keep the number of monitoring wavelengths minimal. However, keeping the number of monitoring wavelengths low means making compromises and not actually using the best monitoring wavelengths for each of the deposited layers.

Here, we propose a different approach to monitoring wavelength selection that also can be fully automated. Instead of searching for one or a few wavelengths for the whole filter stack, we propose to search best wavelength for each layer. Even if it means changing the monitoring wavelength for each of the deposited layers and requires a precise knowledge of the refractive indices as a function of the wavelength. The method we propose is similar to the approach already discussed in [1]: wavelength selection is based on the sensitivity of thickness error to monitoring wavelength. We added to this analysis the noise of monitoring system, the spectral sensitivity to errors in the deposited layer and the spectral sensitivity to errors in previous layers. Additionally, we take into account the technical limitations of optical monitoring systems. To make the monitoring wavelength selection automatic, we first define conditions that would lead to successful deposition for each layer and then select the monitoring wavelengths that match these conditions. As technical limitations, we consider the bandwidth of monitoring signal and the *swing* values. To validate our approach, we perform several experimental demonstrations with increasing complexity of the designed filters.

2. Method

2.1 Technical limitations of optical monitoring

For successful deposition using optical monitoring, it is important to avoid wavelengths that can become the cause for large thickness errors. We have identified several conditions in which a poorly chosen wavelength causes errors, and this wavelength should not be used for optical monitoring. In fact, if certain criteria cannot be fulfilled, optical monitoring will produce larger errors than time monitoring, supposing a constant deposition rate. The wavelength range considered for monitoring is defined by the light source distribution, the detector sensitivity, and the monochromator performances. Also, experience shows that it is advantageous to use wavelengths located in a spectral range corresponding to the application of the filter. Commercially available optical monitoring systems (OMS) are fitted with algorithms that allow online trigger point corrections. These corrections rely on algorithms similar to monitoring by swing values or percent of optical extrema monitoring (POEM) [12,13]. One of the advantages of using POEM-like algorithms is that small deviations of refractive index during deposition can be compensated and layers optical thickness maintained. It is important to have understanding about these algorithms to avoid situations where trigger point correction can increase thickness errors. In case of POEM, deposition is terminated at pre calculated distance from turning points, adjusting the trigger point if measured transmittance at turning points differs from theoretical values. It means that the precision of turning point detection will influence the precision of deposited layer thicknesses.

For thin layers where monitoring wavelengths with turning point cannot be found, time or quartz monitoring is preferred because these adjustments are not possible. Indeed, due to error accumulation, it is possible to reach transmittance level errors, at the beginning of a thin layer deposition, comparable to the total transmittance amplitude variation of the considered layer. Without corrections linked to turning points, relative thickness errors can then reach tens of percent for layers of 20 nm or so thickness. While correction algorithms can use turning points of previous layer for corrections if the same monitoring wavelength is used for several consecutive layers, in this study, we focused on individual layers and did not consider layer pairs for monitoring.

The next parameter to consider is the *start amplitude* - difference between transmittance at the beginning of layer and the first turning point (Fig. 1). Similar criterion for wavelength selection - *swing in* - is described in [2] and Eq 1.We use here the same notations for first and last turning points as in [2], the first turning point for every layer is the one closest to the substrate, and the last is the one closest to air. If the transmittance at the beginning of layer is too close to a turning point, it can result in false detection of the turning point, which can create poor trigger point corrections and create a large thickness error. The false detected turning point can be the result of noisy measurements at the beginning of deposition. This will not be a cause of errors for thick layers with multiple turning points assuming that only first one is detected wrongly. However, for layers with only one turning point this can have a strong impact as an inaccurate correction will be produced. From numerous experiments, we have determined that with our optical monitoring setup configuration, we can use wavelength for optical monitoring only if the *start amplitude* is at least 4%, which is not the same criterion as *Swing in* used in [2]. This shows that there are technical limitations that are not the same for each coater and OMS configuration. For example, signal to noise ratios can vary for different detector and light source pairs. Indeed, even the slit configuration will influence the

noise, because of this we cannot use *swing in* as it is described in [2] but we use *start amplitude* that is relevant our system. It is possible to decrease *start amplitude* by increasing measured signal processing time, however that will have influence on trigger point detection. Longer signal processing time will result in later turning point detection and can create error for trigger point detection.
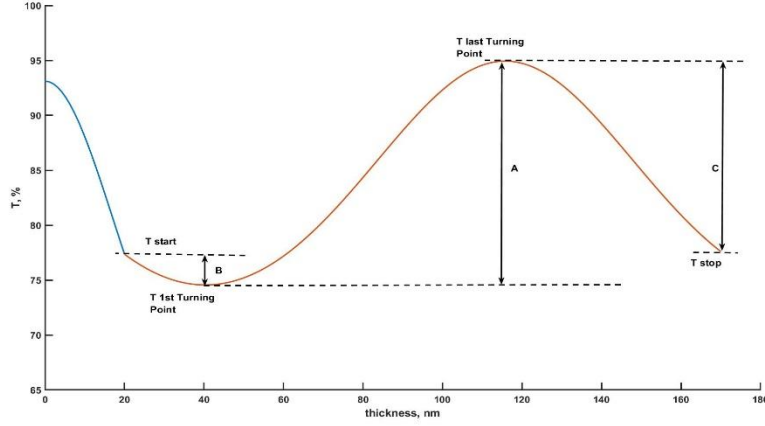

Figure 1 Transmittance evolution versus thickness or 'monitoring curve' of 20 nm Nb_2O_5 layer – blue curve, followed by 150 nm SiO_2 layer -red curve, Monitoring wavelength 450 nm. A – total amplitude – difference between turning points (or maximum and minimum of monitoring signal); B - start amplitude – difference between start transmittance and first turning point; C – final amplitude – difference between last turning point and trigger point.

$$\text{Swing in} = \frac{\left|T_{1st\ TP} - T_{start}\right|}{A}$$

Eq. (1)

$$\text{Swing out} = \frac{\left|T_{last\ TP} - T_{stop}\right|}{A}$$

Eq. (2)

Equations 1 and 2 T_{TP} - transmittance at the last turning point, T_{start} and T_{stop} transmittance at the beginning and end of layer, A - amplitude between the turning points. If there are no (or only one) turning points in layer, the theoretical thickness increase is calculated to find the two extrema.

As for the *start amplitude,* we consider that the *swing out* values are also important. Defined by Eq 2. the Swing out is the ratio of the distance between the last turning point and the trigger point to the total amplitude between the turning points [2]. This parameter is interesting because we want to stop the deposition where the transmittance changes rapidly with increasing thickness. We chose to stop the deposition where the trigger point is in the range of 15-85% of full amplitude. This range is in agreement with previous research by other authors [2] [14]. This forbids all the regions that are close to a turning point. Additionally, based on experience, we include an exception when trigger point is turning point.

The sensitivity of the measured transmittance to the spectral resolution of the monitoring system must also be considered when choosing the monitoring wavelength. Since the bandwidth of the monitoring system (monochromatic) is fixed to a nominal value, we see that it is beneficial to select only wavelengths that are not sensitive to spectral resolution, avoiding sharp spectral peaks. An illustrative example is shown in Fig. 2. Figure 2 (c) is the spectral performance at the end of 28th layer of 2nd monitoring glass from a "*Bonne Mère*" design that is discussed in result section. There are many sharp spectral peaks in 400 - 600 nm wavelength region that will influence the monitoring signal of this layer if wavelength from this range is selected. Indeed, we can show how large is the difference can be between monitoring curves at wavelength λ and average of $\lambda+\Delta\lambda$ representing, as an illustrative example, a 3nm bandwidth. In Fig. 2 (a) and (b) is the monitoring curves with and without bandwidth at two different wavelengths. Not only we see that it is beneficial to select monitoring wavelength where spectral performance after layer do not show high frequency fluctuations of the transmittance, but that in Fig. 2 (a) the differences in maximum and minimum turning points are affected by the spectral resolution of the OMS. If the OMS uses swing values to adjust trigger point value one can expect significant errors when stopping the layer deposition. The required spectral resolution of the monitoring system also depends on the spectral behavior of the manufactured component. In general, a bandpass filter with a given final width FWHM (Full width at Half Maximum) requires a monitoring system with a resolution better than FWHM/5. Otherwise, the deviation between the expected signal and the measured signal can lead to significant thickness errors. Although small spectral resolution can be achieved for most of monochromatic OMS, one generally tries not to diminish it too much to keep best signal to noise ratio. In addition, this can become an important factor if broadband monitoring systems are used as a monochromatic monitoring setup. The bandwidth of BBM is not adjustable and not as good as for monochromatic monitoring setups [6].
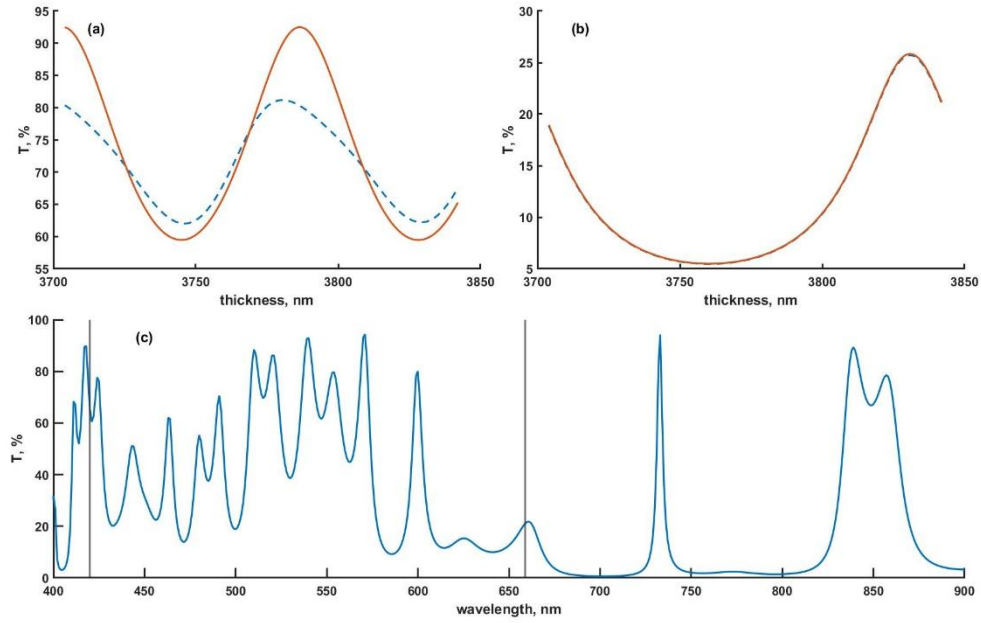
Figure 2 monitoring curves, solid line represents theoretical monitoring curve, dashed line represents theoretical monitoring curve if bandwidth is 3 nm. (a) the monitoring wavelength is 420 nm, (b) 659 nm, (c) spectral performance at the end of the layer, vertical lines are plotted at 420 and 659 nm.

Based on the previously described criteria, in Fig. 3 we have summarized in flowchart the process for determining whether a wavelength can be used for optical monitoring (OM).

We perform binary (yes/no) process for each wavelength in a given spectral range for each layer. In case when no suitable wavelength can be determined for the layer monitoring, we use time monitoring assuming a constant deposition rate calculated from the first deposited layers. If several wavelengths can be used for optical monitoring, we use a merit function to select the optimal monitoring wavelength of each layer.
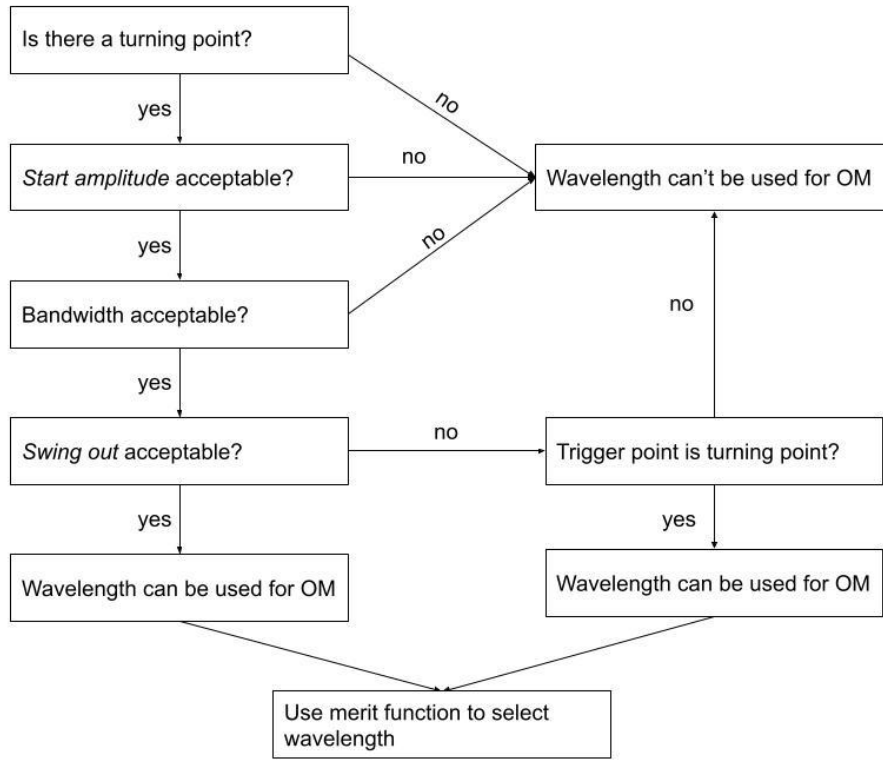
Figure 3. flowchart of the monitoring wavelength selection process

2.2 Merit function to select the monitoring wavelength

In most cases, several wavelengths can meet the technical criteria and we must then select the best one. To do this, we examined the sensitivity of transmittance to thickness as a function of wavelength. If we look at how much the transmittance changes with a small change in thickness, we found that that layer sensitivity can change dramatically from one wavelength to another. This is an important consideration when selecting the monitoring wavelength. Indeed, to increase accuracy, we need to monitor the growth of the layer where a small increase in thickness results in a reliably measurable change in transmittance. Furthermore, if we consider that we have d_n layers referenced as: $d_1,..,d_i,..,d_n$, and there is a potential error in a d_j layer ($j<i$), we should select a monitoring wavelength λ_i for the d_i layer where the error in the d_j layer has a low effect on the monitoring transmittance of the d_i layer. Similarly, it is important to consider the noise of a given optical monitoring system. Selecting a wavelength for measurement where signal to noise ratio is high increases the chances of a successful deposition.

In summary, we highlight 3 important criteria defined for the selection of optical monitoring wavelengths:

1. The stop transmittance value of the layer to be monitored. It is necessary to stop the deposition on a maximum slope at which the transmittance signal evolves significantly with small increases in thickness of the currently monitored layer.
2. The influence of thickness errors of the previous layers. Depending on the design, some spectral regions will undergo greater changes than others with thickness errors. It is therefore advantageous to select the monitoring wavelength in the spectral region where the errors of the previous layers have less effect.
3. The influence of the noise of the monitoring setup at the considered wavelength.

The first and second criteria are sometimes contradictory, so a compromise must be found between them. All these criteria can be summarized in a merit function (MF) with adjustable weighting factors for each of them.

$$MF_i(\lambda) = \frac{1}{\left|\frac{\partial T}{\partial d_i}(\lambda)\right|} * \left[\alpha * \sum_{1 \le j \le i-1}\left|\frac{\partial T}{\partial d_j}(\lambda)\right| + \beta * \Delta T_{NOISE}(\lambda)\right]$$

Eq. (3)

Where T – stands for the transmittance after the deposition of i layers, d_i – is the thickness of the i-th layer, MF_i – is the merit function after deposition of i layers; $\left|\frac{\partial T}{\partial d_i}\right|$ –is the derivative of transmittance with respect to the thickness d_i; ΔT_{NOISE}– is the spectral noise of the monitoring system; α, β –are the weighting coefficients, and λ- the considered wavelength. The noise value was determined at several wavelengths using reference density filters. Its origin is related to the spectral efficiency of the components (quartz halogen light source, Si or PMT detector and slit configuration) of the monitoring device, and also to the dynamic nature of the measurement since the control is located at a radius of ~40 cm from the central axis, and the measurement window is of a duration of about 1 - 1.5 ms.

Theory behind Eq.3 is described in [1], where it is used to evaluate thickness error dependence of monitoring wavelength. We have added noise of monitoring system to initial equation; it is an important factor and can have great impact on precision of trigger point detection.

The monitoring wavelength is then selected by searching for the minimum of the merit function for each layer.

4 merit functions have been considered depending on whether the user wants to favour the influence of the transmittance derivative or the minimization of the noise of the OMS system; the corresponding weighting coefficients are shown in table 1.

Merit function	α	β
MF1	1	0
MF2	0	1
MF3	0.5	0.5
MF4	0.5*	0.5

Table 1 weight coefficients for MFs

For MF4 the sum of the derivatives of the previous layers is replaced by an average of the derivatives of the previous layers (Eq.4).

$$\alpha * \left[\frac{\displaystyle\sum_{1 \le j \le i-1} \left| \frac{\partial T}{\partial d_j}(\lambda) \right|}{i} \right]$$

Eq. (4)

In short, we showed that we select the wavelength for optical monitoring if it passes previously defined criteria. Then we select the best monitoring wavelength for each layer based on the sensitivity to thickness errors, changing the monitoring wavelengths for every layer if necessary. This process can be automated, and the monitoring strategy is selected without the need to manually examine the monitoring curves.

3. Results and discussion

3.1 Experimental setup

Depositions were performed using HELIOS coater and OMS5100 produced by Buhler Leybold Optics. This magnetron sputtering machine is equipped with a rotating turntable where the monitoring sample is placed so as to pass under the magnetron and then under the optical measurement window. The rotation speed is adjusted so that the optical measurement is performed after the deposition of ~0.1 nm of thin film. The layers are deposited by plasma assisted reactive magnetron sputtering [15]. Coatings are deposited using mid frequency dual magnetron configuration from metallic targets and oxidized with radio frequency plasma source. *Ex-situ* spectral measurements are performed with a Perkin Elmer *Lambda 1050* spectrophotometer. Different designs with increased complexity and sensitivity to errors were fabricated. For all of them, we implemented the procedure that we have described above.

The designs presented in this paper were obtained using the commercial software *Optilayer*. The initial solution was usually a single layer whose thickness depends on the complexity of the problem. The needle method allows to quickly obtain a theoretical solution whose number of layers is directly linked to the optical thickness of the initial design. It only remains to eliminate the remaining very thin layers to converge to a feasible solution.

For all the coatings Nb_2O_5 was used as high index material and SiO_2 as low index material. Dispersion curves are plotted in Fig. 4. Fused silica or D263 borosilicate glass were used as substrate. The useful wavelength range for OMS was set at 400 – 900 nm in order to secure optimal signal to noise ratio.
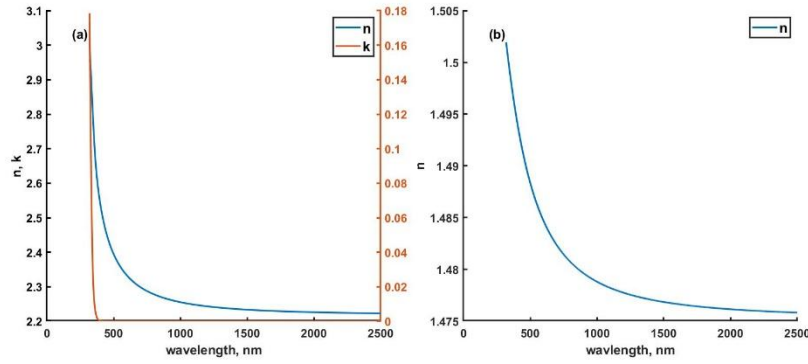
Figure 4 refractive indices of Nb_2O_5 (a) and SiO_2 (b).

3.2 Beam splitter

The first thin film design tested is a 50/50 8-layer beam splitter in the visible range. The layer thicknesses range from 20 to 140 nm (Fig. 5 (b)). For this experiment, wavelengths were selected only by merit functions of Eq.3 at first, and we tested only the idea of selecting different monitoring wavelength for each layer if necessary, without consideration of swing values and bandwidth. The selected monitoring wavelength for different merit functions are shown in table 2.

layer	MF1 (nm)	MF2 (nm)	MF3 (nm)	MF4 (nm)
1	400	603	603	603
2	429	571	552	561
3	575	567	575	575
4	697	569	562	566
5	745	626	745	694
6	840	555	792	550
7	900	484	487	485
8	707	628	677	628

Table 2. monitoring wavelengths resulting from merit function optimization.

As can be seen, MF1 monitoring wavelength for layer 1 is 400 nm and the one for layer 7 is 900 nm. Since it reached the wavelength interval limit, it means that we were not able to reach the minimum of the MF1 and that the proposed strategy is not optimal. Hence, this strategy was not considered for experiments. All the other MF converged with a minimal value resulting in optimal wavelength between 484 and 792 nm. To compare the different merit functions, a standard single wavelength monitoring strategy was also considered. We used the standard approach that consists in analyzing the optical monitoring signals and determining empirically which one appears as the best. In that case, 595 nm was considered as an efficient single monitoring wavelength.
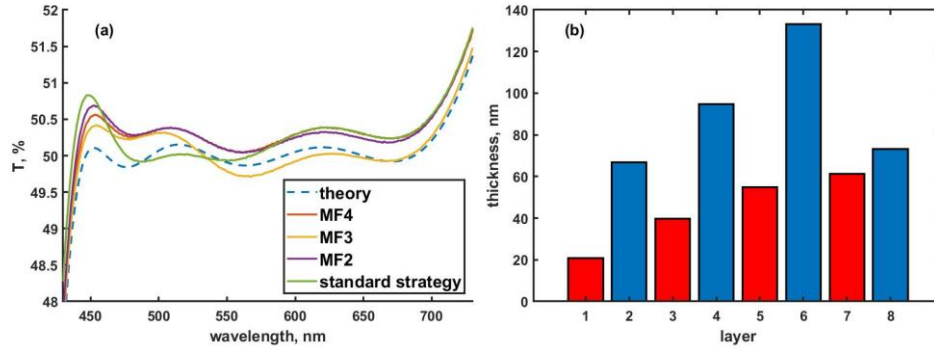
Figure 5. (a) - Measured Transmittance of deposited beam splitters using 3 automated strategies (MF2, MF3, MF4), and single wavelength monitoring (standard strategy) (b) – thicknesses of layers, red bars – high index layers, blue – low index layers.

The results obtained from monitoring with wavelengths selected by different MF minimization shown in Fig. 5 (a) are comparable to those of a carefully selected single wavelength monitoring. It is interesting to note that depending on the implemented strategy, there are systematic errors that will contribute to transmittance deviations that can be large either in blue or red part of the spectrum. However, this first demonstration shows that if the monitoring wavelengths are properly selected, using a different optimized wavelength for each layer is an efficient method for automatic determination of an efficient optical monitoring strategy of the proposed multilayer structure. To validate our approach, more complex designs were studied. Moreover, as it appears that MF4 performed slightly better than the other MF, this criterion was the one used for the remaining part of this study.

3.3 D65 compensation filter

To further test our wavelength selection method, we chose a D65 compensation filter. The standard illuminant D65 represents the spectral distribution of daylight at a color temperature of 6500K [16]. A thin film stack was designed to compensate for the wavelength-dependent illumination of such a source.

The power distribution of D65 illuminant and the corresponding compensating filter are shown in Fig. 6 (a). The power distribution of the standard illuminant is far from smooth and has spectral peaks that cannot be perfectly compensated by thin films filters without significantly increasing the number of layers.

We therefore designed a D65 compensating filter composed of 37 layers that compensates for most of the intensity fluctuations. The layer thicknesses range from 9.0 to 500 nm (Fig. 6 (d)). For selecting the optimal monitoring wavelengths flowchart of Fig. 3 was used and optimal wavelength was selected using MF4.

As with the beam splitter, a standard monitoring strategy was created to be compared to the automatically selected strategy. In this case, it was not possible to find a single wavelength that can be used for all 37 layers. Therefore, the standard strategy was to find a wavelength that can control the most layers and then use time monitoring for the remaining layers. This strategy is possible thanks to the high stability in deposition rates of the magnetron sputtering machine. The selected monitoring wavelength was 400 nm and the first 19 of 37 layers were controlled using optical monitoring. The deposition rates of these layers were then used for the

calibration of the monitoring time of the last layers. For the automatically generated strategy, distribution of monitoring wavelength is illustrated in Fig. 6 (b). Most of the layers are monitored between 550 and 700 nm what corresponds roughly to the spectral region with highest signal to noise ratio for OMS used and only 5 of them are monitored at wavelength below 550 nm. In addition, the monitoring wavelengths could not be found for 5 layers (layers 1, 2,3,5, 23) and were time controlled. For 1st layer, time monitoring was selected because it is a SiO_2 layer, and its refractive index does not have high enough contrast on fused silica substrate for reliable measurement. The other time monitored layers are thin layers (below 20 nm), and monitoring wavelengths that fulfill defined criteria could not be found.
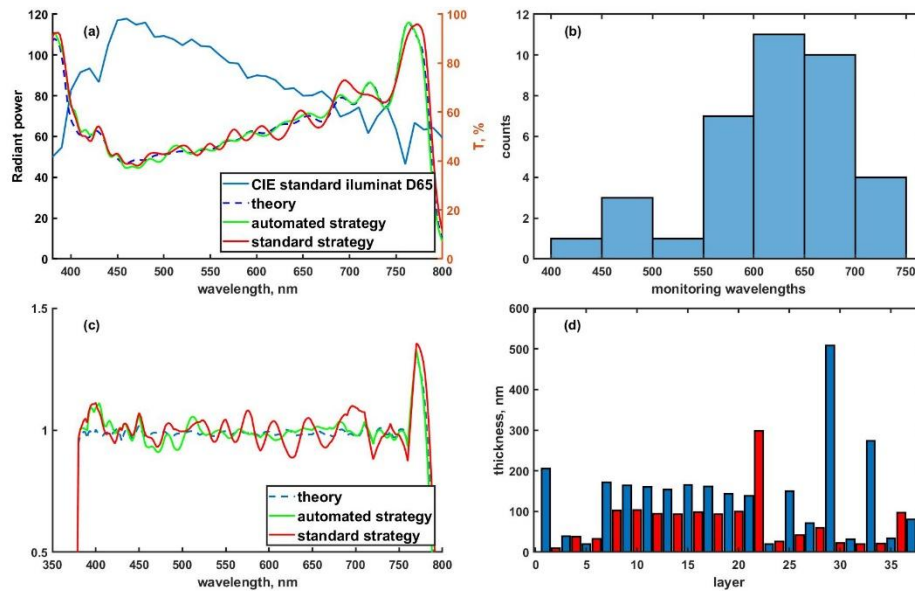

Figure 6. (a) - power distribution of the standard illuminant and theoretical spectral response of the compensating filter and comparison between the theoretical and experimental spectral responses with the automated and standard strategies, (b) – distribution of monitoring wavelengths for automated strategy, (c) – product of the spectral responses of the D65 illuminant by that of the deposited filters. (d) - thicknesses of D65 compensation filter, red - high index layers, blue - low index layers

In Fig 6 (a), the performances obtained with the standard and automated strategies are compared with the theoretical transmittance. It can be seen that the spectral performances of the filters with both strategies are similar at shorter wavelength, but that the automated strategy performs significantly better at longer wavelengths. This is probably due to the fact that the monitoring wavelengths are spectrally spread out (Fig. 6 (b)), whereas only one wavelength (400nm) is used for 'standard' strategy. The use of a second wavelength for standard strategy at longer wavelength could solve this problem but would require additional tests while the automatic strategy only requires one single approach.

The importance of a good spectral match over the entire wavelength range for this filter can be illustrated by multiplying the spectral response of the filter to that of the standard illuminant. In Fig 6 (c) we have confirmation that the performance is similar for both strategies at the

shorter wavelengths, while the automated strategy performs significantly better for longer wavelengths resulting to a flat intensity with one order of magnitude smaller oscillations. In this comparative study, the change of monitoring wavelength therefore appears to provide better results for this filter.

3.4 Notch filter

Another example where wavelengths were selected using our automatic approach is a 98-layer notch filter (Fig. 7 (c)). This filter contains mostly SiO_2 layers that are thinner than 30 nm, and a large number are even thinner than 10 nm. In contrary, the Nb_2O_5 layers are quite thick with thicknesses larger than 150 nm. As can be seen in Fig. 7 (c), except for few layers, this design mostly consists of a thick Nb_2O_5 layer followed by thin SiO_2 layer, a sequence that repeats through most of the design. Since this filter is quite complex, we implemented that classical approach that consists in splitting the deposition into 5 D263 witness glasses used for the monitoring of the whole filter. Here we change witness glass after layer 24, 44, 64 and 84. The choice for changing the witness glass was done arbitrarily every 20 layers or so (to stop on a low refractive index layer). The exact definition of when to change the witness glass remains a challenge that will be the scope of an upcoming study. As discussed earlier in the paper, for layers thinner than 10 nm, time monitoring was systematically used instead of optical monitoring.
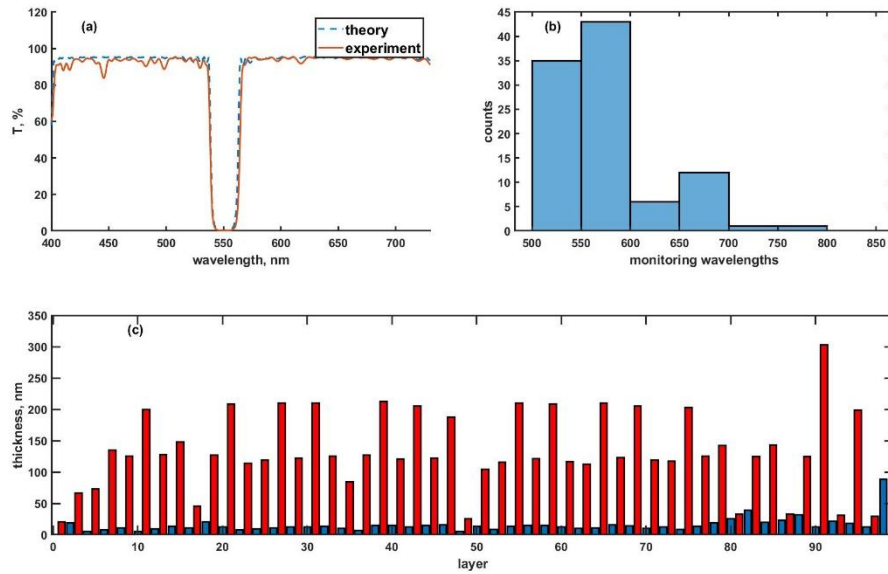

Figure 7. (a) - spectral performance of notch filter, (b)- distribution of monitoring wavelengths (c) - thicknesses of layers, red bars – high index layers, blue – low index layers

Monitoring wavelengths distribution is shown in Fig 7 (b). The selected wavelength are mostly in $500 - 600$ nm range. One of the reasons for this distribution compared to D65 compensator is the high number of thin layers, which monitoring signal shows higher amplitude for shorter wavelengths. Another reason seems to be that because of the thick Nb_2O_5 followed by thin SiO_2 sequence, automatically selected monitoring wavelengths for all witness glasses and layers themselves are similar.

Figure 6 (a) illustrates the performances of the notch filter obtained with the automated strategy. The reflectivity of the notch area is >98% as designed, and the measured bandwidth is 21 nm instead of 20. These performances can be compared with those that have been reported previously [4] with manually selected monitoring wavelengths. We see that a few oscillations with amplitude up to 10% appear on the transmittance reported in this paper that are not present in the one of reference [4]. Such oscillations may be reduced by testing possible different strategies obtained with a different MF or using different coating repartition for the witness glasses. However, as the goal of this paper is to show the potential of this automated approach that does not require extensive effort to provide an efficient optical monitoring strategy, we did not perform further optimization.

3.5 Marseille challenge

For many years, advances in the accuracy of layer control has been demonstrated by reproducing arbitrary profiles [17] such as the shapes of famous buildings or places [18]. To continue this tradition, we present a filter that replicates *la Bonne Mère* - the famous cathedral overlooking Marseille.
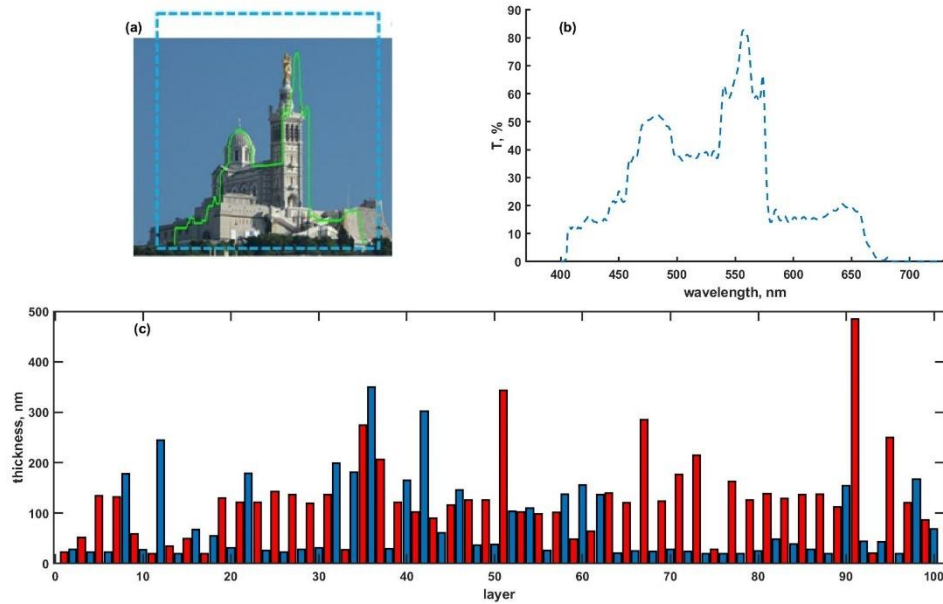

Figure 8. (a) – " la Bonne Mère" (b) *spectral profile from a photograph of "la Bonne Mere"*, (c) thicknesses of "la Bonne Mere" filter, red bars – high index layers, blue – low index layers

The designed filter consists of 100 Nb_2O_5/SiO_2 layers ranging in thickness from 20 to 500 nm (Fig. 8 (c)). As with the D65 compensator, not all the cathedral characteristics can be reproduced without a significant increase in design complexity, and we decided not to reproduce all details that would most probably be washed out with manufacturing errors. We implemented again the strategy consisting in using several witness glasses. Since there is no clear pattern in thickness variations, initially the filter was divided into three parts aiming to have equal number of layers to deposit on each glass. The first two witness glasses have 34 layers and the last one has 32 layers. For each of the three parts, the automated algorithm

described earlier was implemented to select the monitoring wavelengths of each witness glass. Figure 12 (a) shows the optical monitoring wavelength distribution over the three witness glasses. Most of layers are monitored in a range from 550 to 750 nm as for the D-65 compensating filter.
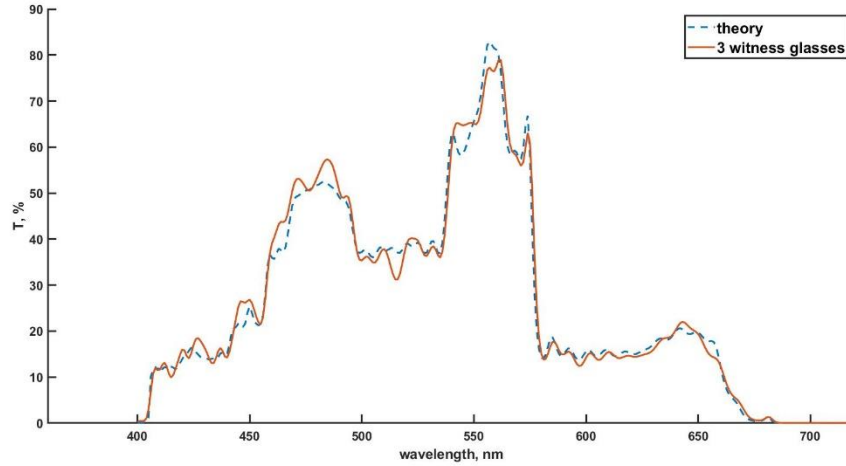
Figure 9. Transmittance as a function of wavelength: comparison between theory and fabrication using 3 witness glasses.

We plotted in Fig. 9, the experimental transmittance that was obtained after fabricating this filter. We observe close agreement between theory and experiment with an average deviation of 2%. It is interesting to note that the best agreement is achieved for wavelengths of 550 nm and above while some additional undesirable ripples are observed at shorter wavelengths. This may be correlated with the monitoring wavelength distribution which are mainly above 550 nm. In addition, one must remember that the determination of the change of the witness glass was done using the criterion of equally distributed number of layers between glasses. We therefore examined the spectral transmittance of the different witness glasses with partial deposition (Fig. 9) to determine how they perform. It is clear that 1st and 3rd glasses show very good agreement between theory and experiment, but the 2nd does not perform as well, especially for wavelengths in 400 - 600 nm range. We wondered whether the criterion of equal number of layers from one witness glass to another is a good approach to divide layers between witnesses.
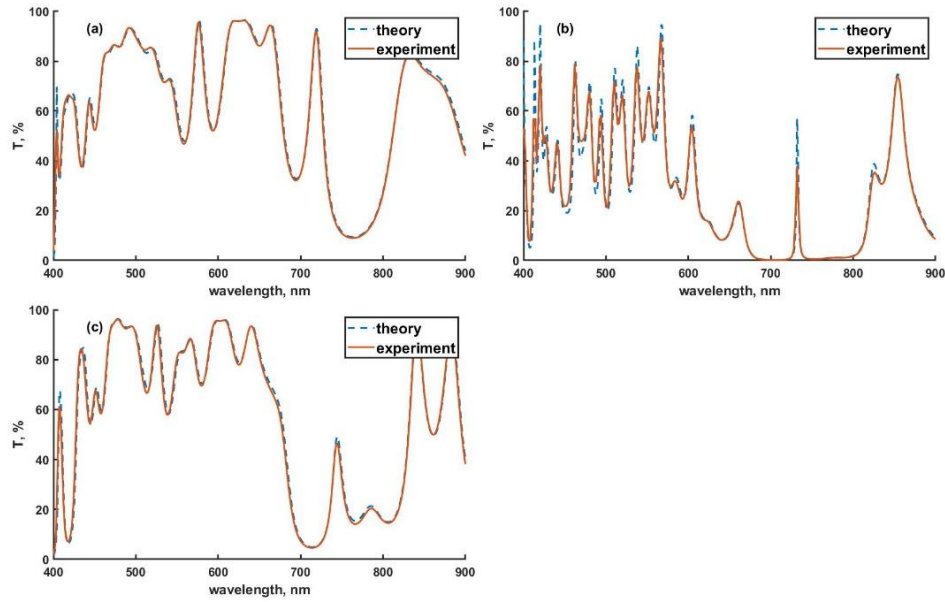
Figure 10. Measured transmittance of each witness glass compared to theory, (a) -witness glass 1, (b) – 2, (c)-3

Indeed, as can be seen in Fig. 8 (c) there are several layers thicker than 200 nm between layers 35 and 68 making the total optical thickness of the 2nd witness glass noticeably higher than others. To take into account this observation, we decided to divide the stack into 4 parts, with similar optical thickness on each of the witness glasses. Since a good agreement between measured spectra and theory was achieved on the 1st witness glass, the optical thickness of it was used as a target thickness when dividing layers. Now witness glass was changed after layer 34, 52 and 80 and the automatic selection of wavelengths was performed for each of the sub-stack. Figure 12 (b) shows that wavelength distribution on all witness glasses. Interestingly, the wavelength spread is larger than in the case of 3 witness glasses with a largest contribution between 500 and 700 nm.
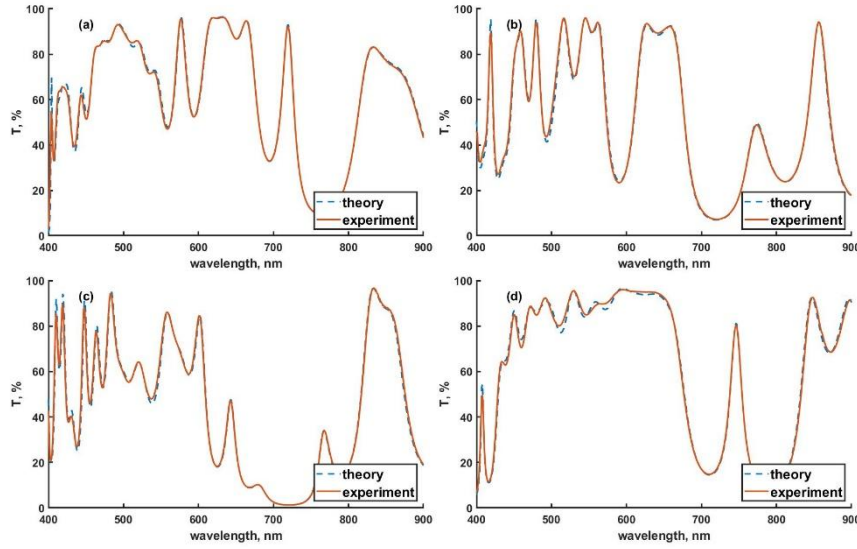
Figure 11. measured transmittance of each witness glass compared to theory, (a) -witness glass 1, (b) – 2, (c) – 3,(d) – 4

We plotted in Fig. 11 the theoretical and experimental transmittance of each of the 4 witness glasses. Splitting the monitoring into 4 parts clearly improved the spectral performance of each individual witness glass with only very minimal deviation, not exceeding a few percent. We finally plotted in Fig. 13, the spectral performance of the witness glass that was coated with all the layers. Surprisingly, the proposed new strategy did not improve the final filter performance (Fig. 13) and even degraded it. This indicates that increasing the number of witness glasses is not enough to improve the final result as even if each individual witness glass performs better, there are no correlation and error compensation between each witness glass. This result reinforces the need to study and determine the optimal conditions for changing a witness glass when coating complex filters.
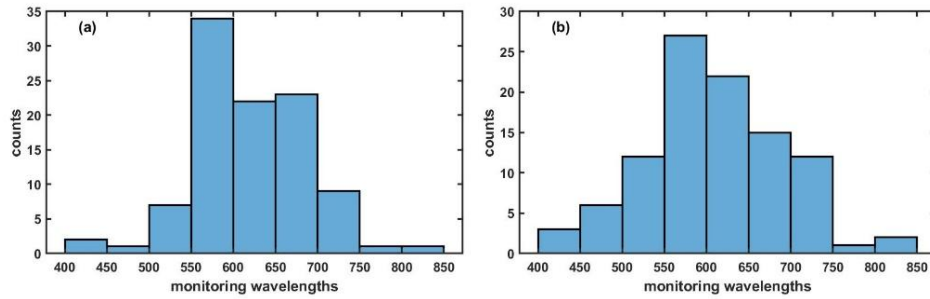

Figure 12 wavelength distribution for Bonne Mère design (a) - for 3 witness glasses, (b) – for 4 witness glasses

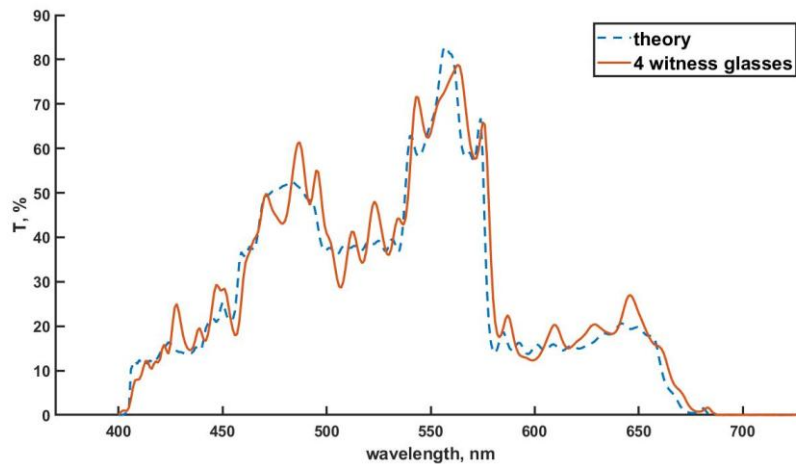*Figure 13. spectral performance of la Bonne Mère using 4 witness glasses.*

4. Conclusions

We have proposed an automated method for selecting the monitoring wavelength of each layer of multilayer structures. The monitoring wavelengths must meet certain criteria that we have detailed, otherwise the optical monitoring will introduce large thickness errors. If a suitable monitoring wavelength cannot be found, it is best to use time monitoring for that particular layer. Such an approach was demonstrated on different filters with various complexities. Can this method be successfully implemented for different deposition methods remains to be validated. Sputtering in general, and magnetron sputtering in particular, are known to be very stable deposition processes. Deposition rates with electron beam deposition processes are much more erratic. In this case, time monitoring seems to be a very poor monitoring criteria. Another advantage of magnetron sputtering is the stability of the refractive index, which is mandatory for a multi-wavelength monitoring approach like the one performed in this paper.

We also showed that for more complex structures, several witness glasses can be used to avoid the accumulation of thickness errors. However, exactly where to change the witness glasses remains a difficult question, with a trade-off between global (the whole filter) and partial (the witness glass with partial coating) error compensation. Despite this difficulty that needs further study, we have shown that our method allows automatic wavelength selection approach for successful control and fabrication of complex thin film components with performances comparable to best hand-determined optical monitoring strategies.

Funding

Disclosure

The authors declare that there are no conflicts of interest related to this article.

Data availability

Data underlying the results presented in this paper are not publicly available at this time but may be obtained from the authors upon reasonable request.

References

1. A. V. Tikhonravov, M. K. Trubetskov and T. V. Amotchkina, "Statistical approach to choosing a strategy of monochromatic monitoring of optical coating production," Appl. Opt. **45**, 7863–7870 (2006).

2. M. Trubetskov, T. Amotchkina and A. Tikhonravov, "Automated construction of monochromatic monitoring strategies," Appl. Opt. **54**, 1900 (2015).

3. P. Bousquet, A. Fornier, E. Pelletier and P. Roche, "Optical filters: Monitoring process allowing the auto-correction of thickness errors," Thin Solid Films **13**, 285–290 (1972).

4. A. Zöller, M. Boos, R. Goetzelmann, H. Hagedorn, B. Romanov and M. Viet, "Accuracy and error compensation with direct monochromatic monitoring," Opt. InfoBase Conf. Pap. 1–3 (2013).

5. T. Begou, F. Lemarchand, F. Lemarquis, A. Moreau, T. Begou, F. Lemarchand, F. Lemarquis, A. Moreau and J. Lumeau, "High performance thin-film optical filters with stress compensation," J. Opt. Soc. Am. A Opt. Image Sci. Vision, Opt. Soc. Am. C121. hal-02350443 (2019).

6. O. Lyngnes, U. Brauneck, J. Wang, R. Erz, S. Kohli, B. Rubin, J. Kraus and D. Deakins, "Optical monitoring of high throughput ion beam sputtering deposition," Opt. Syst. Des. 2015 Adv. Opt. Thin Film. V **9627**, 962715 (2015).

7. B. Badoil, F. Lemarchand, M. Cathelinaud and M. Lequime, "Interest of broadband optical monitoring for thin-film filter manufacturing," Appl. Opt. **46**, 4294–4303 (2007).

8. A. Tikhonravov, I. Kochikov, I. Matvienko, T. Isaev and A. Yagola, "Strategies of broadband monitoring aimed at minimizing deposition errors," Coatings **9**, (2019).

9. A. Zoeller, H. Hagedorn, W. Weinrich and E. Wirth, "Testglass changer for direct optical monitoring," Adv. Opt. Thin Film. IV **8168**, 81681J (2011).

10. A. Zöller, D. Arhilger, M. Boos and H. Hagedorn, "Advanced optical monitoring system using a newly developed low noise wideband spectrometer system," Opt. Syst. Des. 2015 Adv. Opt. Thin Film. V **9627**, 1–5 (2015).

11. L. Li and Y. Yen, "Wideband monitoring and measuring system for optical coatings," Appl. Opt. **28**, 2889–2894 (1989).

12. R. R. Willey, "Simulation comparisons of optical monitoring strategies in narrow bandpass filters," Opt. InfoBase Conf. Pap. **53**, 27–34 (2013).

13. A. Macleod, *Thin Film Optical Coatings*, 4th ed. (CRC /Taylor & Francis Group, 2010).

14. R. R. Willey, "Preserving Error Compensation Benefits While Changing Monitoring

Wavelengths with Each Layer," 3–9 (2016).

15.   M. Scherer, "Magnetron sputter-deposition on atom layer scale," Vak. Forsch. und Prax. **21**, 24–30 (2009).

16.   N. Ohta and A. R. Robertson, *CIE Standard Colorimetric System* (2006).

17.   D. Poitras, L. Li, M. Jacobson and C. Cooksey, "2019 Topical Meeting on Optical Interference Coatings: Manufacturing Problem Contest [invited]," Appl. Opt. **59**, A31–A39 (2019).

18.   B. T. Sullivan and J. A. Dobrowolski, "Deposition error compensation for optical multilayer coatings II Experimental results—sputtering system," Appl. Opt. **32**, 2351 (1993).